

All-optical mode unscrambling on a silicon photonic chip

Francesco Morichetti¹, Andrea Annoni¹, Stefano Grillanda¹, Nicola Peserico¹, Marco Carminati¹, Pietro Ciccarella¹, Giorgio Ferrari¹, Emanuele Guglielmi¹, Marc Sorel², and Andrea Melloni¹

¹*Dipartimento di Elettronica, Informazione e Bioingegneria, Politecnico di Milano, via Ponzio 34/5, 20133 Milano, Italy*

²*School of Engineering, University of Glasgow, Glasgow, G12 8LT, UK*
francesco.morichetti@polimi.it

Abstract

We demonstrate a 4-channel silicon photonic MIMO demultiplexer performing all-optical unscrambling of four mixed modes. Mode unscrambling is achieved by means of a cascaded Mach-Zehnder architecture that is sequentially reconfigured by individually monitoring each stage through integrated transparent detectors, namely Contact Less Integrated Photonic Probes (CLIPPs). Robust demultiplexing of 10 Gbit/s channels with less than -20 dB crosstalk is achieved.

1. Introduction

Mode-division multiplexing (MDM) is now considered a promising approach to boost the capacity of optical fiber transmission [1]. However, such a new paradigm requires optical components capable to manipulate signals encoded on different orthogonal modes and mixed after propagation through a multimode link. Multiple-input multiple output (MIMO) photonic integrated architectures realizing reconfigurable mode (de)multiplexing and unscrambling have been recently proposed [2] and realized [3]. In these schemes the possibility to monitor individual channels multiplexed in the MDM signal is an essential feature to enable simple and robust tuning strategies. However, channel monitoring in MDM systems must be non-invasive in order to preserve mode orthogonality.

In this work we demonstrate all-optical unscrambling of four-mixed modes on a silicon photonic (SiP) chip. We exploit transparent photodetectors, realized through the non-invasive ContactLess Integrated Photonic Probe (CLIPPs) technology [4], to monitor the evolution of the modes intensity along a MIMO demultiplexer, without impairing mode orthogonality. Demultiplexing of 10 Gbit/s channels with less than -20 dB residual crosstalk is demonstrated.

2. Design and fabrication

Figure 1(a) shows a schematic of the realized 4-channel all-optical MIMO demultiplexer, according to the architecture concept proposed in Ref. 2. After propagation and mutual mixing

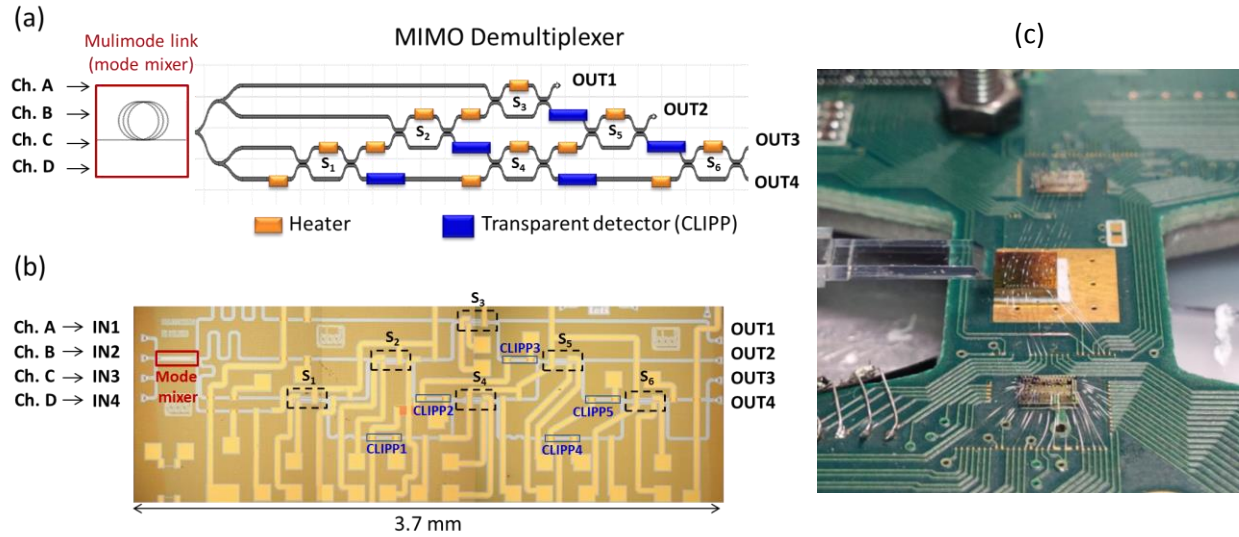


Fig. 1: (a) Schematic and (b) top-view microphotograph of the 4-channel MIMO demultiplexer realized on a SiP platform. A multimode waveguide is used to induce mode mixing of the input channels (A,B,C,D). (c) Photograph of the SiP chip wire-bonded to a readout CMOS electronic ASIC and integrated onto the same printed circuit board. A glass based transposer is used to couple the four channels into the SiP circuit.

through a multimode link, four optical channels (Ch. A – Ch. D) are coupled into four single-mode optical waveguides. As a result, each waveguide typically brings a portion of the light intensity of each input channel. The all-optical MIMO demultiplexer consists of an arrangement of 6 interferometric switching stages (S_i , $i = 1, 2, \dots, 6$), realized through integrated Mach-Zehnder Interferometers (MZIs), that can be sequentially tuned in order to reconstruct and arbitrarily extract each channel at each output port (OUT1–OUT4). For instance, to demultiplex Ch. x ($x = A, B, C, D$) at port OUT1, stages S_1 , S_2 and S_3 need to be sequentially biased in order to minimize Ch. x power at the output lower branch of each stage. Transparent detectors are needed to monitor the switching state of each stage without introducing optical loss that would impair mode orthogonality.

The 4-channel MIMO demultiplexer was realized on a 220-nm SiP platform through LETI-ePIXfab multi-project-wafer run. A top-view photograph of the Si chip is shown in Fig. 1(b). A pair of thermal actuators are integrated in each switching stage S_i to control the relative phase of the optical field at the input ports and between the inner arms of each MZI. The switching state of each MZI is individually monitored real time with a CLIPP detector integrated at one output port. Mode mixing of input channels Ch. A – Ch. D is performed on chip through a mode mixer realized with a multimode waveguide section. As shown in Fig. 1(c), the four channels are coupled to the SiP through a glass based transposer [5] enabling to inject the signals coming from four single-mode-fibers to four input grating couplers. The SiP chip is mounted on PCB and bridged to a

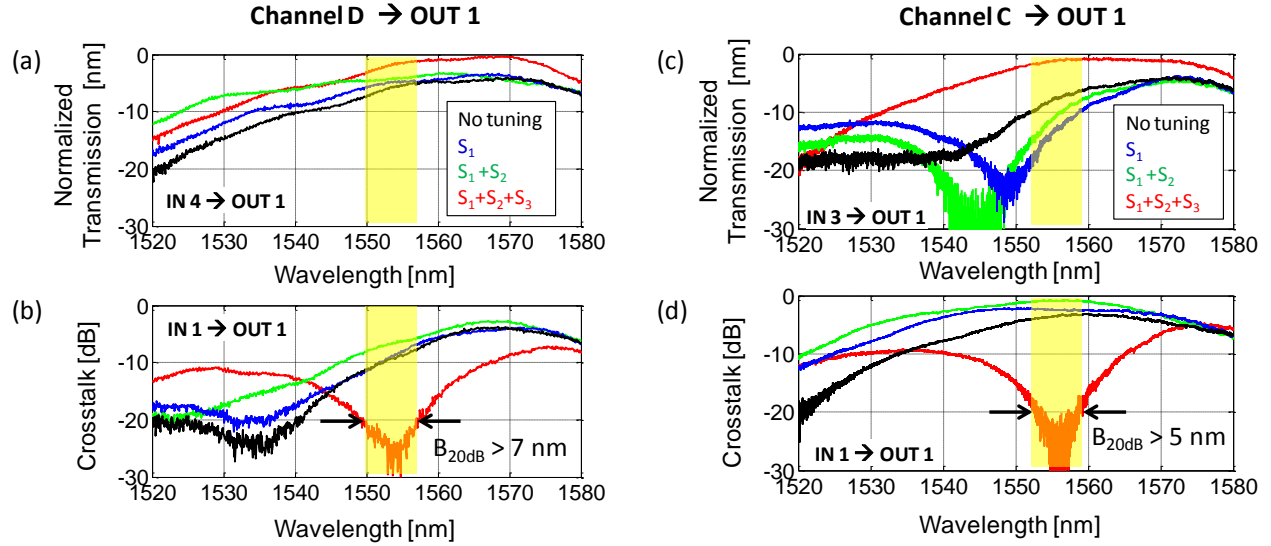


Fig. 2: Measured frequency domain response of the 4-channel MIMO demultiplexer. In (a) and (b) the circuit is sequentially tuned to extract Ch. D ($\lambda_D = 1555$ nm, input port IN4) from OUT1: (a) transmission spectra IN4 \rightarrow OUT1 and (b) crosstalk spectra IN1 \rightarrow OUT1 (due to Ch. A) measured in the as-fabricated device (no tuning, black), after tuning of stage S_1 (blue), of stage S_2 (green) and of stage S_3 (red). Panels (c) and (d) show the circuit tuning to extract Ch. C ($\lambda_C = 1555$ nm, input port IN3) from OUT1: (c) transmission spectra IN3 \rightarrow OUT1 and (d) crosstalk spectra IN1 \rightarrow OUT1 (due to Ch. A).

CMOS electronic ASIC, enabling simultaneous read out of the integrated CLIPPs and providing the driving voltage for the thermal actuators [6].

3. Experimental results

Figure 2 shows the measured frequency domain response of the 4-channel MIMO SiP demultiplexer. As a first case analysis, we consider the extraction from output port OUT1 of Ch. D injected at port IN4 and centered around a wavelength $\lambda_D = 1555$ nm. Measurements performed on an identical mode mixer realized onto the same chip reveal that at this wavelength, at least 20% of the light intensity of each channel is distributed at each single-mode input waveguide of the demultiplexer. Sequential MZI tuning is performed by minimizing the light intensity of Ch. D at the lower output branch of stages S_1 - S_3 by using CLIPPs 1-3, respectively. Weak modulation tones (kHz frequency range) are added to each input channel to enable each CLIPP of the circuit to identify individual channels regardless of the presence of other channels [7]. Figure 2(a) shows the transmission spectra from IN4 to OUT1 when all the thermal actuators are off (black curve), after tuning stage S_1 (blue), stage S_2 (green) and stage S_3 (red). It can be noted that the signal detected at the output port OUT1 does not monotonically increase with the number of tuned stages; this prevents from the possibility of using information on OUT1 power level for circuit configuration, and confirming the need for on-chip intensity monitors. In the

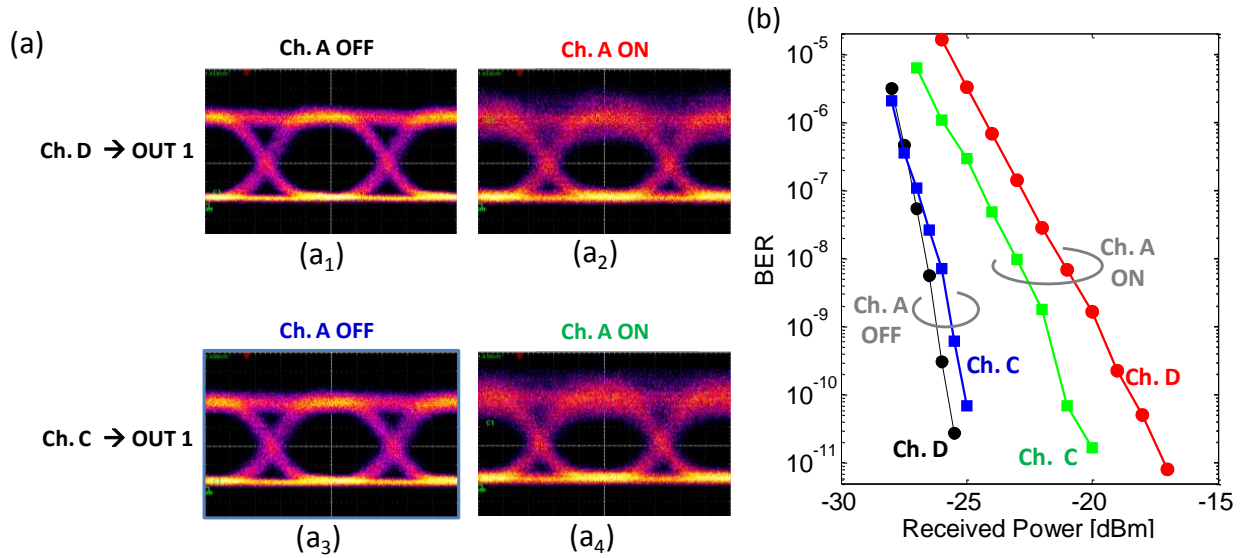


Fig. 3: (a) Measured eye diagrams of mode demultiplexed 10 Gbit/s OOK NRZ signals. Eye diagram of Ch. D (IN4) extracted at port OUT1 (a₁) in absence and (a₂) in presence of Ch. A (IN1). Eye diagram of Ch. C (IN3) extracted at port OUT1 (a₃) in absence and (a₄) in presence of Ch. A (IN1). (b) BER of demultiplexed Ch. C and D when Ch. A is switched off (blue and black) and when Ch. A is switched on (red and green).

tuned device, transmission maximum is around 1568 nm, because of the wavelength-dependent efficiency of the vertical grating couplers. Figure 2(b) shows the crosstalk spectra measured in the same tuning conditions of Fig. 2(a) due to Ch. A injected from input port IN1. Around 1555 nm, a crosstalk of less than -20 dB is achieved on a bandwidth $B_{20\text{dB}}$ of more than 7 nm, the rejection bandwidth being mainly limited by the wavelength dependence of the MZI directional couplers. As another example, Figs. 2(c) and (d) show the circuit tuning to extract Ch. C ($\lambda_C = 1555$ nm) injected at port IN3 from the same output port OUT1. Again, mode demultiplexing is achieved with less than -20dB crosstalk from input IN1. Similar performances were observed on other IN-OUT port combinations.

Figure 3 shows the eye diagrams and the bit-error-rate (BER) of the demultiplexed channels in the cases considered in Fig. 2. Two 10 Gbit/s OOK NRZ channels sharing the same carrier wavelength of 1555 nm are achieved by splitting and decorrelating through a few-km-long fiber coil the data stream generated from a 10G Cisco SFP+ module. As a first experiment, we injected the two signals respectively at ports IN1 (Ch. A) and IN4 (Ch. D) of the 4-channel demultiplexer with the same power level of 0 dBm. The eye diagram of Ch. D extracted at the output port OUT1 is shown when Ch. A is switched off (a₁) when Ch. A is switched on (a₂). Despite a slight signal quality degradation due to -20 dB residual crosstalk, a good eye-opening is preserved. As shown in Fig. 3(b), power penalty compared to the reference performance (Ch. A off, black curve) is about 6 dB (red curve) at a BER level of 10⁻⁹ and about 3 dB at a BER level of 10⁻⁶.

Likewise, when the two 10 Gbit/s signals are injected as Ch. A and Ch. C, a slight degradation of the eye diagram is observed on Ch. C demultiplexed at the output port OUT1; power penalty compared to the reference performance (Ch. A off, blue curve) is less than 4 dB (green curve) at a BER level of 10^{-9} and less than 2 dB at a BER level of 10^{-6} .

4. Conclusion

We demonstrated a 4-channel SiP photonic MIMO demultiplexer performing all-optical unscrambling of four mixed modes. On-chip light monitoring through transparent CLIPP detectors was exploited to achieve accurate and robust sequential tuning of the demultiplexer without affecting mode orthogonality, thus enabling demultiplexing of 10 Gbit/s channels with less than -20 dB crosstalk over a bandwidth of more than 5 nm. CLIPP-assisted sequential would allow to increase the port count of the MIMO demultiplexer without increasing tuning complexity in proportion. Further, scalability to channels with different modulation formats and higher bit rates is expected.

Acknowledgment

The authors acknowledge support of the EU Project BBOI (www.bboi.eu) of the 7th EU Framework Program. We acknowledge L. Livietti from Polifab (<http://www.polifab.polimi.it/>) for help in the mechanical assembly of the experimental setup.

References

- [1] P. J. Winzer, "Making spatial multiplexing a reality," *Nat. Photon.* **8**, 345-348 (2014).
- [2] D. A. B. Miller, "Self-configuring universal linear optical component," *Photon. Res.* **1**, 1-15 (2013).
- [3] N. K. Fontaine, "Space division multiplexing and all-optical MIMO demultiplexing using a photonics integrated circuit," *Proceed. Optical Fiber Communication Conference (OFC 2012)*, Los Angeles (CA), 4–8 March 2012, paper PDP5B.1
- [4] F. Morichetti, *et al.*, "Non-invasive on-chip light observation by contactless waveguide conductivity monitoring," *IEEE J. Sel. Topics Quantum Electron.* **20**, 292-301 (2014).
- [5] For details on the glass transposer technology, refer to the website: <http://www.plconnections.com/documents/ICE%20R020815.pdf>
- [6] S. Grillanda *et al.* "Non-invasive monitoring and control in silicon photonics using CMOS integrated electronics," *Optica* **1**, 129-136 (2014).
- [7] S. Grillanda *et al.*, "Hitless monitoring of wavelength and mode-division multiplexed channels on a silicon photonic chip," *Proceed. Optical Fiber Communication Conference (OFC 2015)*, Los Angeles (CA), 22–26 March 2015, paper W1A.3.